

ОБЪЕДИНЕННЫЙ
ИНСТИТУТ
ЯДЕРНЫХ
ИССЛЕДОВАНИЙ
ДУБНА

A 89

E13-88-892

A.Yu.Astakhov, Yu.A.Batusov, Gy.L.Bencze, I.Farago,
A.Kisvaradi, L.Molnar, L.M.Soroko, J.Vegh

MESOOPTICAL FOURIER TRANSFORM
MICROSCOPE – A NEW DEVICE
FOR HIGH ENERGY PHYSICS

Submitted to "NIM, A"

1988

INTRODUCTION

Owing to an excellent spatial resolution the traditional nuclear emulsion technique remains until recently the most powerful, convenient and sometimes the only conceivable particle detector, particularly in the experiments with particles of very short lifetime ($10^{-18} \div 10^{-10}$ s)^{/1/}. Typically, a nuclear emulsion particle detector has a form of the solid block of volume up to 50 liters composed of many 0.6 mm thick pellicles. The dimensions of each pellicle are 100 mm x 200 mm. Going through this emulsion block charge particles leave their tracks in the form of straight lines consisting of small silver grains $0.5 \div 1 \mu\text{m}$ in size with linear density of grains for relativistic particles of the order of $20 \div 30$ pro $100 \mu\text{m}$.

The experimental setup is usually equipped with different external particle detectors and a spectrometer by means of which the location of a nuclear event in the nuclear emulsion block can be estimated with spatial uncertainties of $2 \div 3$ mm. As the volume to be examined is still of the order of 0.1 cm^3 , the $6 \div 8$ emulsion layers of the post processed thickness 0.2 mm must be looked through to find the predicted event. To distinguish the dots of the particle track of the dimension $0.5 \div 1 \mu\text{m}$, a very high geometrical magnification is needed to find these tracks. As the depth-of-focus of the optical microscope is of the order of $3 \div 5 \mu\text{m}$, each emulsion layer must be subdivided into 50 separate images to be investigated. The speed of the manual search is of the order of 1 cm^2 per day and the probability of success is not more than 30%.

Several attempts have been made to automatize the search and to decrease the time needed by increasing the probability of success and by saving observers from hard and tiresome work. The most natural way is to digitize the image produced by the optical microscope, to supply the microscope table with motors and position encoders and to connect everything to a computer. Such equipment was built in different laboratories, e.g. the ICANS (Interactive Computer Aided Measurement System) in the Lawrence Berkeley Laboratory^{/2/} and in the measuring centre of the Nagoya University^{/3/}. These apparatus are suitable for measuring rather than finding the events. The time required

to find an event was reduced by using an external emulsion sandwich in the E-531 experiment in the Fermi National Accelerator Laboratory^{/3/}. An equipment called CADIM (Computer Aided Digitized Microscope) was built in CERN^{/4/} to make the search easier by giving an artificial picture of tracks predicted by the external detectors. This picture could be compared with the real image. Making decisions, however, remains the operator's task.

Despite considerable progress achieved by these systems they have two basic disadvantages due to the fact that the primary objects of observation are the dots which form the particle track: 1) a very complicated computation process or operator's decision is needed to decide whether the dots form a real particle track or not; 2) the depth-of-focus problem remains unsolved.

To find a solution to these problems the key element of the equipment, namely the optical microscope, had to be changed. A few years ago a completely new idea called Mesooptical Fourier-Transform Microscope (MFTM) was put forward^{/5/}. This microscope sees only straight particle tracks of the width comparable with the light wave length and spreads out all particle tracks according to their orientations with the speed of light. The depth scanning in the MFTM is completely withdrawn. Meanwhile the information about the Z-coordinate of the particle track is not lost in the MFTM. Actually, in this new device two mesooptical images are produced at two different camera angles. All these advantages have been achieved experimentally by introducing in the MFTM the mesooptical imaging unit instead of the traditional optical objective and by the fundamental changing of the object illumination system.

After several years of investigations on the development of the MFTM a computer controlled system of observation with MFTM as the main unit was built^{/6-12/}. Some theoretical and experimental works on mesooptics and mesooptical microscopes were carried out during this period^{/13-22, 24-29/}.

In this paper we describe the Mesooptical Fourier Transform Microscope (MFTM) and the computer controlled system with the MFTM as the main unit for the fast search for particle tracks in nuclear emulsion. Some results of the early experimental tests of the system are presented and discussed. It is shown that the angular resolution of the MFTM is equal to 1 angular minute and the measurement time is equal to 30 ms. As all operations in the MFTM are going on without any depth scanning and without any Z-control our searching system works at least two orders of magnitude faster than any known system with a traditional optical microscope.

THE PRINCIPLE OF THE MFTM

The schematic optical diagram of the MFTM is given in fig.1^{/8-9/}. The convergent beam of light produced by the Fourier lens 1 illuminates the nuclear emulsion layer 2. The crossover of this convergent beam of light is in the vicinity of the mesooptical mirror with the ring response 3. The term mesooptic was introduced in^{/20/}. The imaging element is called a mesooptical one if in the frame of geometrical optics approximation the point in the object space is transfor-

Fig.1. The schematic optical diagram of the Mesooptical Fourier Transform Microscope (MFTM): 1 - Fourier Transform lens, 2 - nuclear emulsion layer, 3 - mesooptical mirror with ring response, 4 - two particle tracks (A and B) which cross each other within the field of view of MFTM; A_L and A_R - mesooptical images of the particle track A, B_L and B_R - mesooptical images of the particle track B.

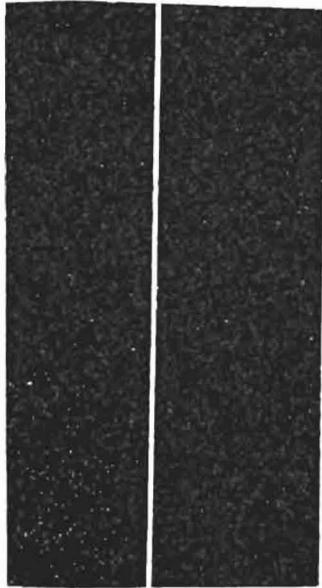
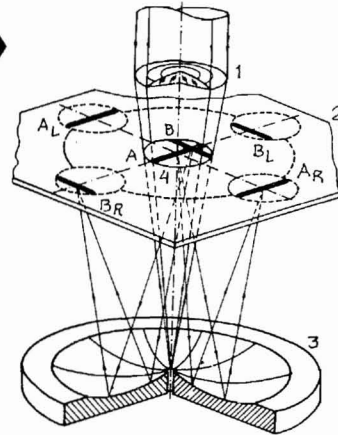


Fig.2. Part of the focal circle produced by the mesooptical mirror with ring response with point light source placed in the first focus of the ellipse.

med into a straight or curved line of finite dimensions in the image space. In a general case the n -dimensional object is transformed into an $(n+1)$ - or $(n+2)$ -dimensional image^{/9/}.

Each straight particle track produces a far field diffraction pattern in the form of a bright straight line strip of width equal to the diameter of the convergent beam crossover. The undiffracted light goes through the central hole in the mesooptical mirror 3. The axial symmetrical mesooptical mirror 3 has an elliptical radial profile. The first common focus of these ellipses is on the optical axis while the second focuses of the ellipses form a focal circle. The fragment of the focal circle produced by the mesooptical mirror 3 which was illuminated by a point light source is shown in fig.2. The width of this focal circle is equal to $1.5 \mu\text{m}$, whereas the diffraction limited width is $1.4 \mu\text{m}$ ^{/11/}.

The problem of the depth focus is solved in the MFTM without loss of the radial resolution in the meridional cross section of the MFTM. The profile of the mesooptical mirror 3 has the form of a polygon with many elements, the length of which is equal to $100 \mu\text{m}$ that is of the order of the depth of the nuclear emulsion layer, corrected by the refraction of the light.

Each particle track consisting of dark points on the bright illuminated field is transformed by the MFTM into two bright illuminated mesooptical images on the semidark background: the left one (L) and the right one (R). The straight line connecting two mesooptical images of the given particle track is perpendicular to the direction of this track. Two particle tracks, A and B, which cross each other within a field of view of the MFTM, are transformed into two pairs of mesooptical images, A_L and A_R for A, and B_L and B_R for B, which lie in completely different parts of the focal circle. This "automatic" spreading of the mesooptical images of the particle tracks in accordance with their orientations is the main feature of the MFTM. The locus of all mesooptical images forms a ring of width D and of average radius R_0 (fig.3), where D is the diameter of the field of view of the MFTM^{/17/} and R_0 is the radius of the focal circle.

Each particle track which goes parallel to the median plane of the nuclear emulsion layer is determined by three coordinates: the orientation angle θ , the distance ρ_0 from the optical axis and by its Z-coordinate with $Z=0$ in the median plane of the nuclear emulsion layer (fig.4). As is seen from this figure, we have

THE PRINCIPLE OF THE MFTM

The schematic optical diagram of the MFTM is given in fig.1^{/6-9/}. The convergent beam of light produced by the Fourier lens 1 illuminates the nuclear emulsion layer 2. The crossover of this convergent beam of light is in the vicinity of the meso-optical mirror with the ring response 3. The term meso-optic was introduced in^{/20/}. The imaging element is called a meso-optical one if in the frame of geometrical optics approximation the point in the object space is transfor-

Fig.1. The schematic optical diagram of the Meso-optical Fourier Transform Microscope (MFTM): 1 - Fourier Transform lens, 2 - nuclear emulsion layer, 3 - meso-optical mirror with ring response, 4 - two particle tracks (A and B) which cross each other within the field of view of MFTM; A_L and A_R - meso-optical images of the particle track A, B_L and B_R - meso-optical images of the particle track B.

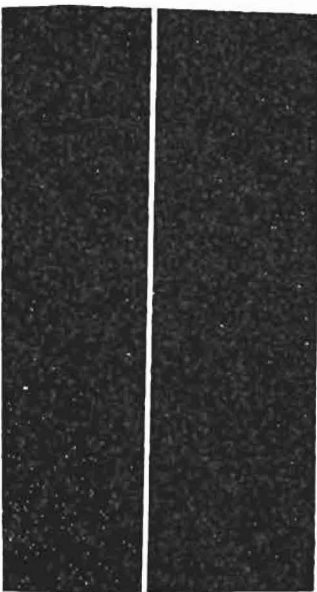
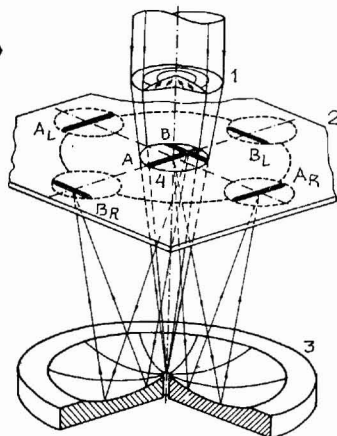


Fig.2. Part of the focal circle produced by the meso-optical mirror with ring response with point light source placed in the first focus of the ellipse.

med into a straight or curved line of finite dimensions in the image space. In a general case the n -dimensional object is transformed into an $(n+1)$ - or $(n+2)$ -dimensional image^{/9/}.

Each straight particle track produces a far field diffraction pattern in the form of a bright straight line strip of width equal to the diameter of the convergent beam crossover. The undiffracted light goes through the central hole in the meso-optical mirror 3. The axial symmetrical meso-optical mirror 3 has an elliptical radial profile. The first common focus of these ellipses is on the optical axis while the second focuses of the ellipses form a focal circle. The fragment of the focal circle produced by the meso-optical mirror 3 which was illuminated by a point light source is shown in fig.2. The width of this focal circle is equal to $1.5 \mu\text{m}$, whereas the diffraction limited width is $1.4 \mu\text{m}$ ^{/11/}.

The problem of the depth focus is solved in the MFTM without loss of the radial resolution in the meridional cross section of the MFTM. The profile of the meso-optical mirror 3 has the form of a polygon with many elements, the length of which is equal to $100 \mu\text{m}$ that is of the order of the depth of the nuclear emulsion layer, corrected by the refraction of the light.

Each particle track consisting of dark points on the bright illuminated field is transformed by the MFTM into two bright illuminated meso-optical images on the semidark background: the left one (L) and the right one (R). The straight line connecting two meso-optical images of the given particle track is perpendicular to the direction of this track. Two particle tracks, A and B, which cross each other within a field of view of the MFTM, are transformed into two pairs of meso-optical images, A_L and A_R for A, and B_L and B_R for B, which lie in completely different parts of the focal circle. This "automatic" spreading of the meso-optical images of the particle tracks in accordance with their orientations is the main feature of the MFTM. The locus of all meso-optical images forms a ring of width D and of average radius R_0 (fig.3), where D is the diameter of the field of view of the MFTM^{/17/} and R_0 is the radius of the focal circle.

Each particle track which goes parallel to the median plane of the nuclear emulsion layer is determined by three coordinates: the orientation angle θ , the distance ρ_0 from the optical axis and by its Z-coordinate with $Z=0$ in the median plane of the nuclear emulsion layer (fig.4). As is seen from this figure, we have

Fig.3. The coordinate systems for input and output signals of the MFTM: a) polar coordinate system (r, θ) which defines the position of the particle track within the field of view; b) coordinate system (θ, ρ_1, ρ_2) which defines the position of the two meso-optical images (L and R) at the output of the MFTM.

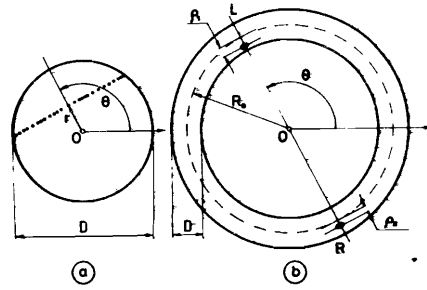
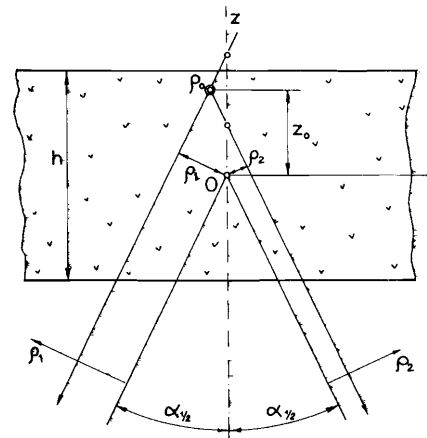


Fig.4. The cross section of the nuclear emulsion layer of the thickness h by the plane perpendicular to the straight line particle track with ρ_0 and z_0 as coordinates of the particle track in this cross section; $\alpha_{1/2}$ is the angle between the central ray of the diffracted light and the optical axis of the MFTM.



$$z_0 = \frac{1}{2} \frac{\rho_1 + \rho_2}{\sin \alpha_{1/2}},$$

$$\rho_0 = \frac{1}{2} \frac{\rho_1 - \rho_2}{\cos \alpha_{1/2}},$$

(1)

where ρ_1 and ρ_2 are the "visible" distances from the centre of the fields of view for the left and right meso-optical images^{17/}, and $\alpha_{1/2}$ is the angle between the central ray of the diffracted light and the optical axis of the MFTM. The deep angle θ_z which the particle track forms relative to the median plane of the nuclear emulsion layer can be measured by the MFTM as well.

Fig.5. The sagittal cross section of the nuclear emulsion layer with particle track AB which lies in the median plane of the nuclear emulsion layer. The end points of this track produce two focal circles of the same radius of curvature R .

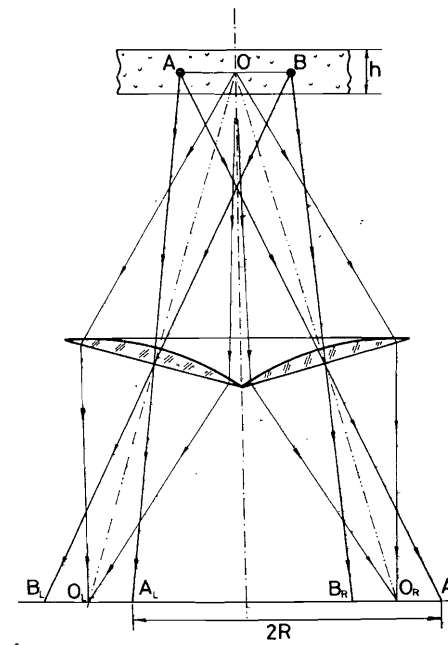


Fig.6. The view of two focal circles of the particle track with end points A and B. The cross points are on the line which is perpendicular to track AB.

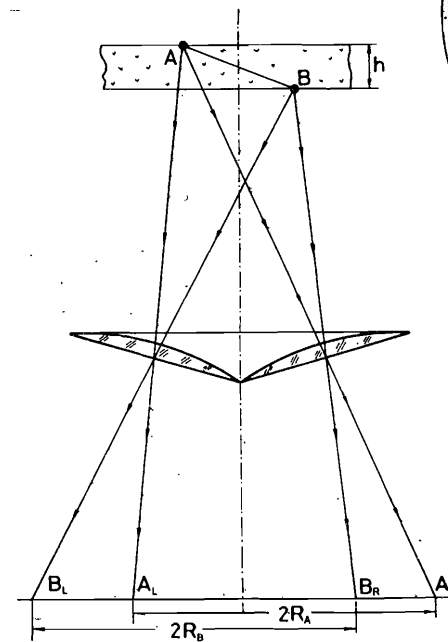
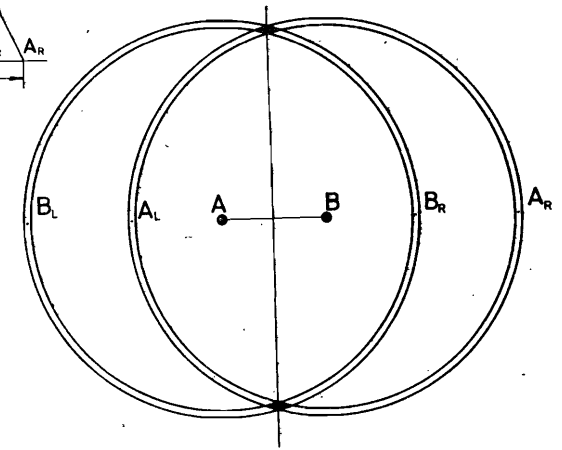


Fig.7. The sagittal cross section of the nuclear emulsion layer with particle track AB with $\theta_z \neq 0$. The radii of two focal circles are different: $R_A \neq R_B$.

Fig.8. The view of two focal circles of the particle track shown in fig.7. The cross points are on the line which does not cross the optical axis of the MFTM.

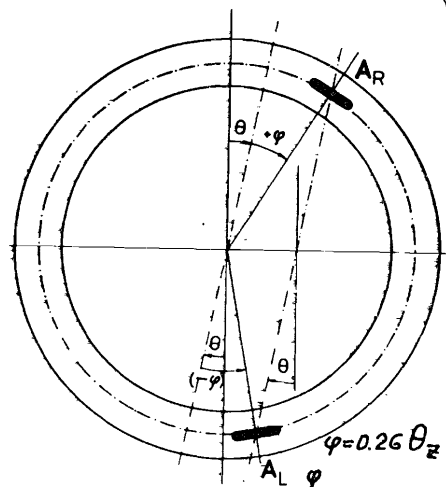
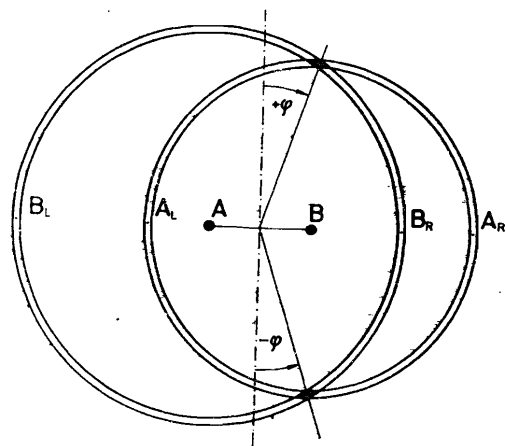


Fig.9. The focal ring of the MFTM and the position of two meso-optical images of the particle track with deep angle $\theta_z \neq 0$.

To understand the influence of the deep angle θ_z on the position of the meso-optical images of a given particle track let us consider the end points of this particle track (fig.5). Each point produces its own focal circle, and the cross-points of two focal circles are on the line which goes through the optical axis of MFTM (fig.6). If the particle track forms a deep angle θ_z with the median plane of the nuclear emulsion (fig.7), the radii of two focal circles of two end points will be different. Due to this the line which connects two meso-optical images of the given particle track does not go through the optical axis of the MFTM (fig.8). However, it goes parallel to the line, on which there are the meso-optical images of the particle track with the same θ_{xy} and with $\theta_z = 0$ (fig.9). The deep angle θ_z is determined by the angle ϕ .

Thus all four parameters which define the position of the particle track in space (θ_{xy} , ρ_0 , z_0 , θ_z) can be estimated

by the MFTM without any displacement of the object and without the stage of receiving the information about individual silver grains of the particle track. The absence of any depth scanning, both mechanical and electrical, is the second main feature of the MFTM.

The theory of the MFTM was treated in ref.^{/13-20/}. As is shown in ref.^{/14/}, the convolution kernel of the MFTM is the spatial derivative of the Dirac delta plus (or minus) function:

$$h(\rho) = \frac{d}{d\rho} \delta_{\pm}(\rho),$$

with

$$\delta_{\pm}(\rho) = \frac{1}{2} \delta(\rho) + \frac{P}{i2\pi\rho}, \quad (2)$$

where $\delta(\rho)$ is the Dirac delta function and P indicates that the convolution integral is taken in the sense of the Cauchy principal value^{/23/}. Relation (2) was corroborated experimentally in ref.^{/24/}, where it was shown that the meso-optical system with the ring response does indeed accomplish the spatial differentiation along the radial coordinate. Due to this the large dark disk is transformed by the MFTM into two concentric fine focal circles the width of which is determined by the numerical aperture of the meso-optical mirror with the ring response.

REAL CONSTRUCTION OF THE MFTM

As is seen from fig.1, two meso-optical images of the straight line particle track are produced within the nuclear emulsion layer. This is of course a drawback of such configuration. There are also two additional problems which must be solved prior to reading out the information about the positions of the meso-optical images: 1) there are no picture detectors with a spatial resolution of the order of $1 \mu\text{m}$; 2) two meso-optical images are separated by a very large distance. In the real construction of the MFTM both these problems are solved in the optical interface with two arms, one for the left meso-optical image and the other for the right meso-optical image. This two-arm optical interface gives an optical magnification along the radial coordinate and puts together two meso-optical images within the frame of one CCD matrix^{/25/}.

Fig.10. The meridional cross section of the two-arm optical interface of the MFTM: 1 - nuclear emulsion layer, 2 - meso-optical mirror with ring response, 3 - rotating platform, 4 - plane mirrors, 5 - corner mirror, 8 - view of the CCD matrix.

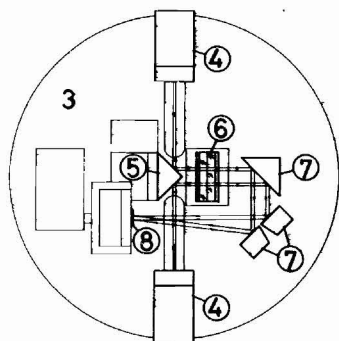
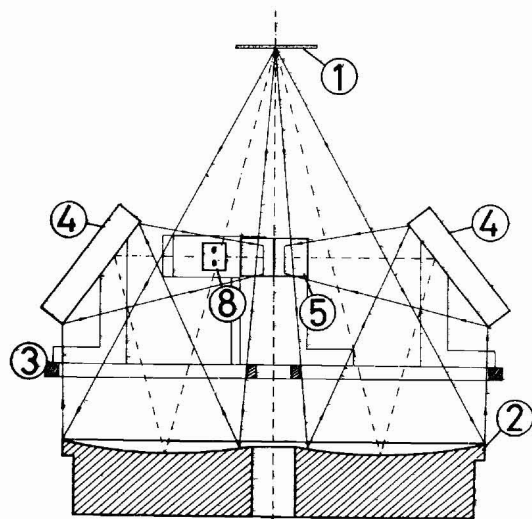


Fig.11. The top view of the two-arm optical interface of the MFTM: 4 - plane mirrors, 5 - corner mirror, 6 - negative cylindrical lens, 7 - plane mirrors, 8 - CCD matrix.

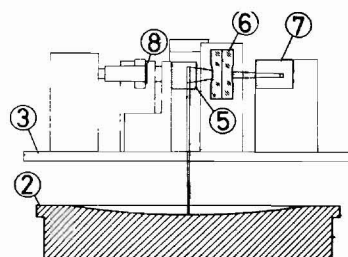


Fig.12. Sagittal view of the two-arm optical interface of the MFTM: 2 - meso-optical mirror with ring response, 3 - rotating platform of the optical interface, 5 - corner mirror, 6 - negative cylindrical lens, 7 - plane mirrors, 8 - CCD matrix.

This two-arm optical interface as is seen in the meridional cross section of the MFTM is shown in fig.10. The top and sagittal views of this unit are given in fig.11 and fig.12. The light diffracted on the straight line particle track in the nuclear emulsion layer 1 going perpendicular to the plane of fig.10 is concentrated into a very thin strip in the vicinity of the meso-optical mirror 2, practically in the plane of fig.10. All other parts of the meso-optical mirror remain dark. One part of the diffracted light is reflected by

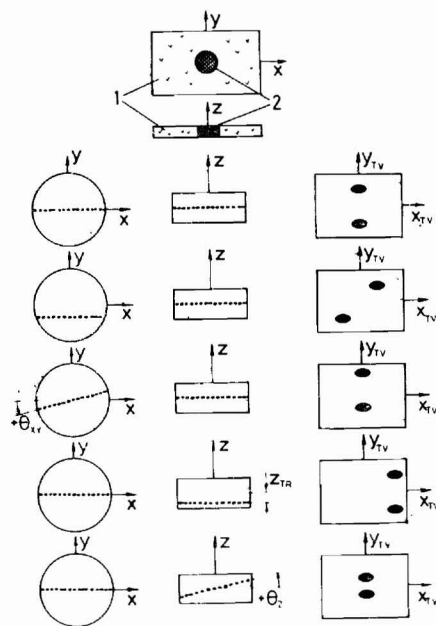
the meso-optical mirror 2 to the left and the other one to the right. These two components of the diffracted light are reflected successfully from the plane mirrors 4, corner mirror 5 and go through the common negative cylindrical lens 6. The last plane mirrors 7 direct these two components of the diffracted light onto one CCD matrix 8. The operator sees two bright spots on the dark of the TV-screen, whenever a particle track is in the field of view of the MFTM. In one possible configuration chosen in our construction the left meso-optical image is at the top of the screen and has the coordinates x_{TV}^L , y_{TV}^L , whereas the right meso-optical image is at the bottom of the screen and has the coordinates x_{TV}^R , y_{TV}^R . Thus we can statically estimate four coordinates of two meso-optical images of a given particle track.

If the particle track crosses the optical axis of the MFTM, two spots on the TV-screen are at points with $x_{TV}^L = x_{TV}^R = 0$ (fig.13). Two spots produce antisymmetrical configuration with $x_{TV}^L + x_{TV}^R = 0$ if the particle track is at some nonzero distance from the optical axis. In both cases the particle track is in the median plane of the nuclear emulsion layer. Two spots of the particle track which has the orientation angle $\theta_{xy} \neq 0$ relative to the orientation of the two-arm optical interface move up, if $\theta_{xy} > 0$, and move down, if $\theta_{xy} < 0$. If the particle track is at the bottom of the nuclear emulsion layer, its meso-optical spots are on the right side of the TV-screen and, finally, two spots which belong to the particle track with depth inclination angle $\theta_z \neq 0$, are closer to each other, if $\theta_z > 0$, and more widely separated, if $\theta_z < 0$. The general view of the two-arm optical interface of the MFTM is shown in fig.14.

Now we may list the operations which are carried out in the MFTM simultaneously without any consumption of time:

- 1) selection of straight line particle tracks in nuclear emulsion, the width of a track being no more than $3 \div 5 \mu\text{m}$, all other wider objects are partially or completely suppressed in intensity;
- 2) reading out 3D information about the position of the straight line particle track in space, including its Z-coordinate without any scanning operations;
- 3) selection of straight line particle tracks in accordance with orientation angle θ_{xy} and deep angle θ_z ;
- 4) well interpreted stereoscopic display of geometrical data in the compressed digital form;
- 5) amelioration of the signal-to-noise ratio only for straight line particle tracks.

Fig.13. The behaviour of the two meso-optical images on the TV-screen in some typical situations: 1 - nuclear emulsion layer, 2 - field of view, x, y - coordinates of the points on the nuclear emulsion layer, x_{TV}, y_{TV} - coordinates of the points on the TV-screen, the position of the particle track is determined by four coordinates: $x_{TR}, y_{TR}, \theta_{xy}, \theta_z$.



Besides these operations the following problems can be solved by using the above-mentioned compressed digital data and the meso-optical Moire-like effect which offers additional scopes of the MFTM ^{/26/}:

- 1) measurement of the scattering angles in the "kink" or "fook" events ^{/26/};
- 2) estimation of the position of the vertex of the event in the field of view of the MFTM ^{/27/} and even outside ^{/17,28/};
- 3) estimation of the curvature radius of the quasistraight particle tracks ^{/29/};
- 4) estimation of the small decay length of the short-lived particle ^{/28/}.

THE COMPUTER CONTROLLED MFTM

The aim of the computer controlled MFTM is to find the particle track according to the predetermined values of angles θ_{xy} and θ_z within the given restricted regions in several (5 ÷ 10) nuclear emulsion layers. The functional scheme of the computer controlled MFTM is shown in fig.15. The light source 1 is a 5 mW He-Ne laser. The lens 2 with focal length $f = 400$ mm accomplishes 2D spatial Fourier Transformation of the particle track. As shown in ref. ^{/15/}, the grain structure of the straight line particle track does not alter the intensity of the main diffraction maximum and only gently changes the intensity of side-lobes. As all particle tracks with the same θ_{xy} but with different θ_z , lie in the same vertical plane, we can supplement the illumination system with a positive cylindrical lens 4, which increases the density of light and the signal-to-noise ratio as well. The lens holder 5 can be rotated together with the rotating platform 12 of the two-arm optical interface. The field of view is about 0.7 mm along the particle track and about 50 μm across it. The negative cylindrical lens 10 magnifies the width of the meso-optical images from 2 μm to 50 ÷ 200 μm . Two meso-optical images of a particle track are picked up by one common CCD matrix 11. A 232x144 element CCD matrix with dimensions of one pixel 21x27 μm was used.

The X-Y stage 7 is equipped with DC motors and Moire-type position encoders with 2.5 μm steps. The platform 12 of the two-arm optical interface is rotated by a DC motor, its position is controlled by a 4000 step rotating encoder.

The electronical part of the equipment is shown in fig.16. The whole system is controlled and the output data are col-

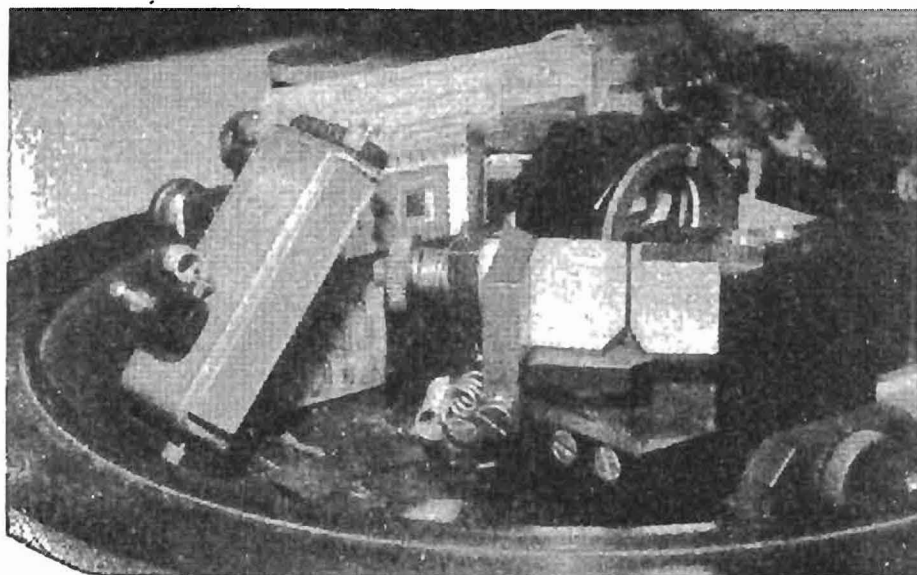


Fig.14. The photo of the two-arm optical interface of the MFTM with negative cylindrical lens in the centre of the photo and CCD matrix to the left.

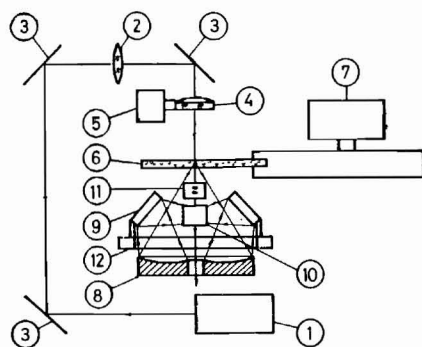


Fig. 15. The functional scheme of the computer controlled MFTM: 1 - laser, 2 - Fourier Transform lens, 3 - plane mirrors, 4 - positive cylindrical lens, 5 - rotating lens holder, 6 - nuclear emulsion layer, 7 - motorized stage equipped with position encoders, 8 - meso-optical mirror with ring response, 9 - plane mirrors, 10 - negative cylindrical lens, 11 - CCD TV-camera, 12 - rotating platform of the two-arm optical interface.

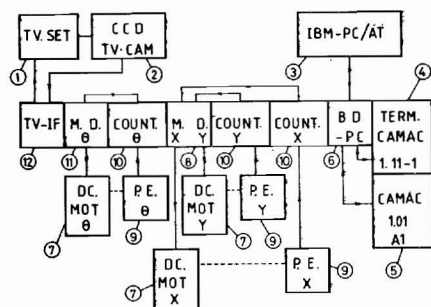


Fig. 16. The electrical part of the computer controlled MFTM: 1 - standard TV set, 2 - CCD TV camera, 3 - personal computer IBM-PC/AT, 4 - branch terminator, 5 - crate controller A1, 6 - branch driver personal computer interface, 7 - direct current motors X, Y, 8 - motor driver double block X-Y, 9 - position encoders X, Y, 10 - counters X, Y, 11 - motor driver, 12 - TV interface.

lected by an IBM PC AT type personal computer. The PC is connected to the equipment through a one-crate CAMAC system which consists of different blocks: counters, motor drivers and a TV-block. The counters 10 are connected to the position encoders of the X-Y stage and of the rotating platform and count the absolute movements of all these stages. The motor drivers 11 make the stages move smoothly at different speed. The TV block 12 consists of a comparator which produced a binary picture of the meso-optical images given by the CCD matrix and converts this picture into a compressed digital form. The level of the comparison can be changed by the computer. The general view of the whole computer controlled MFTM is shown in photo 17.

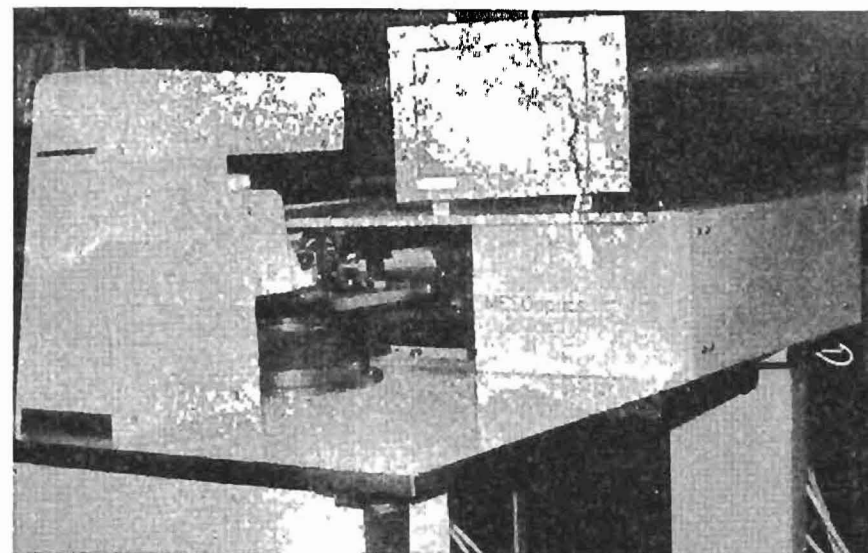


Fig. 17. General view of the computer controlled MFTM (JINR, Dubna).

EXPERIMENTAL CONDITIONS

The nuclear emulsion layer to be examined is put into X-Y stage. The stage moves to the starting point of the area to be examined. The rotating platform of the two-arm optical interface and the illuminating cylindrical lens holder are set to the given angle θ_{xy} . Then the whole area is scanned along the lines separated approximately by a distance of about half size of the field of view. The scanning lines are perpendicular to the direction of the particle track to be searched for. After each step of this scanning the X-Y stage stops and there is no particle tracks at the given angular interval $\theta_{xy}^0 - \delta\theta_{xy} < \theta_{xy} < \theta_{xy}^0 + \delta\theta_{xy}$, where $2\delta\theta_{xy}$ is the accepted angular range of the whole system, the stage moves to the next stop. If any picture exists, then the positions of the stage X_0, Y_0 and the TV picture in the compressed digital form are recorded in the PC. After finishing the scanning along many scanning lines over the whole area we can turn the rotating platform and the cylindrical lens holder to the next angular interval and repeat the scanning. At

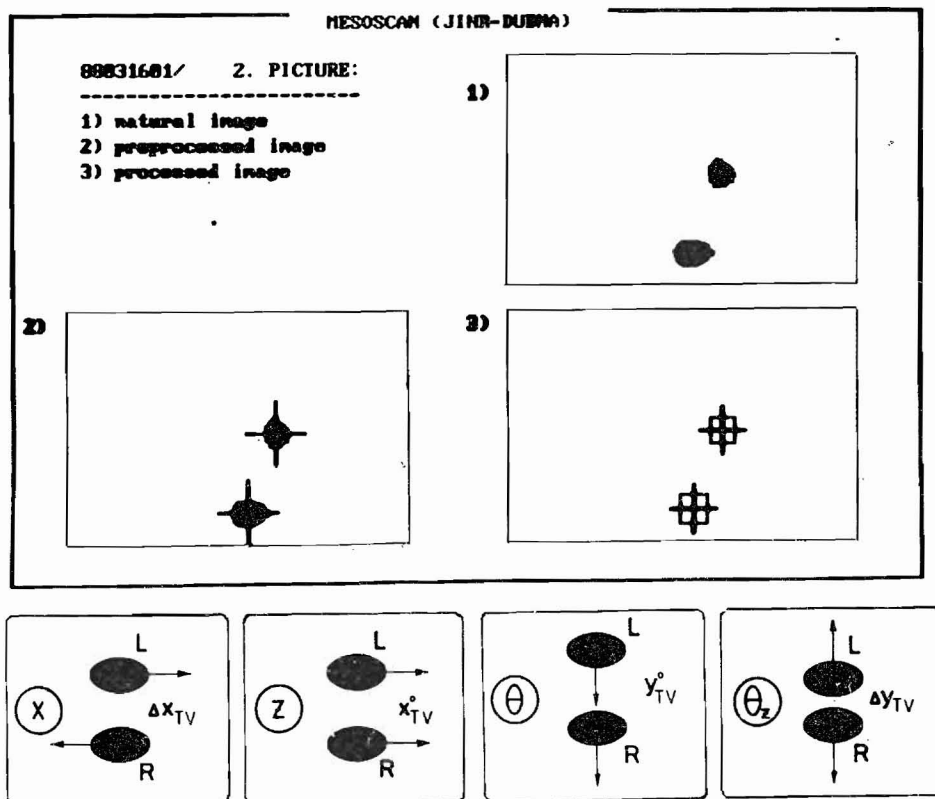


Fig.18. Mesooptical signals on the TV-screen and the explanatory key (very bottom).

the end of this scanning process the whole necessary information is stored in the memory of the PC.

The evaluation of the recorded data consists of two independent steps. At the first step the exact TV coordinates x_{TV}^L , y_{TV}^L , x_{TV}^R , y_{TV}^R of the mass centres of the spots are found in each picture recorded. Then using the calibration data for four coordinates x , z , θ_{xy} and θ_z and the recorded X-Y and angle data four coordinates of the particle track registered at the given X-Y position of the stage are found.

In fig.18 top right are the initial mesooptical images of the particle track on the TV-screen, bottom left are the filtered data with marks showing the position of the mass centres of the spots, and, finally, bottom right are the rectangulars with all mesooptical images inside.

EXPERIMENTAL RESULTS

The part of the nuclear emulsion which was examined by the computer controlled MFTM is shown in fig.19. The particle tracks were produced by strong ionizing neon nuclei accelerated by the JINR synchrophasotron up to the impulse of 4.5 GeV/c per nucleon. An area 6x6 mm in size with almost parallel tracks was scanned along the lines approximately perpendicular to the tracks. The distance between the scanning lines was 0.5 mm, the distance between two subsequent stops

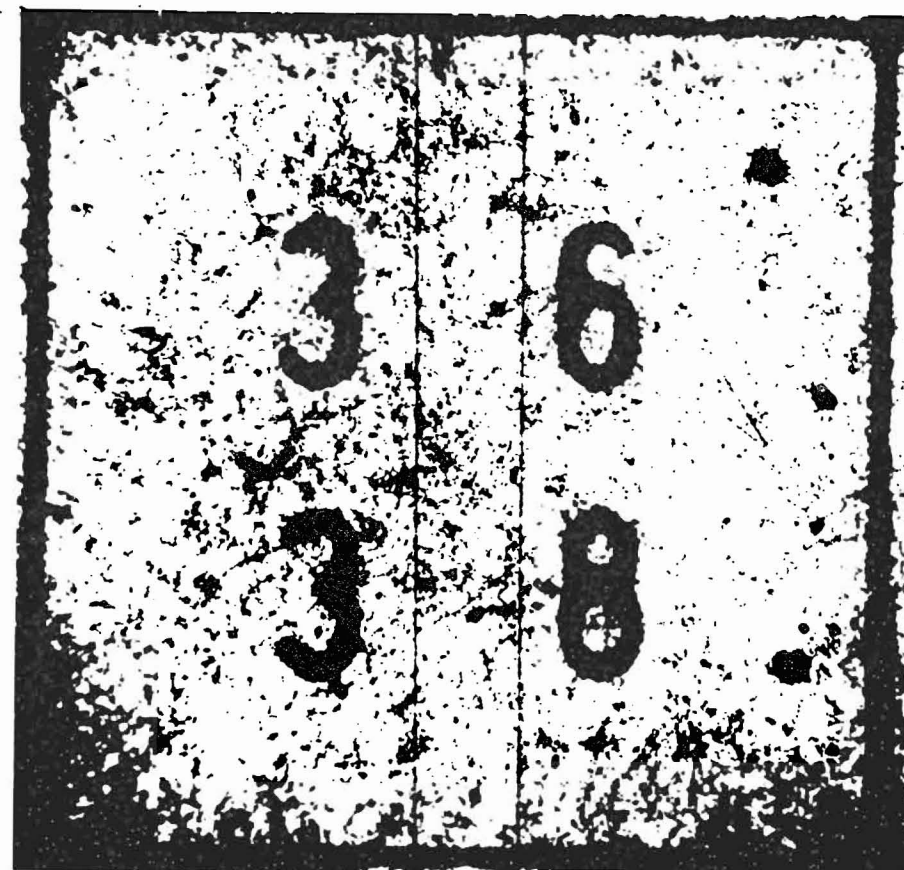


Fig.19. A part of the nuclear emulsion layer marked by the grid with X-ray. The width of the grid is 10 μm , the period is 1 mm.

Fig.20. The positions of 8 particle tracks found and measured by the computer controlled MFTM.

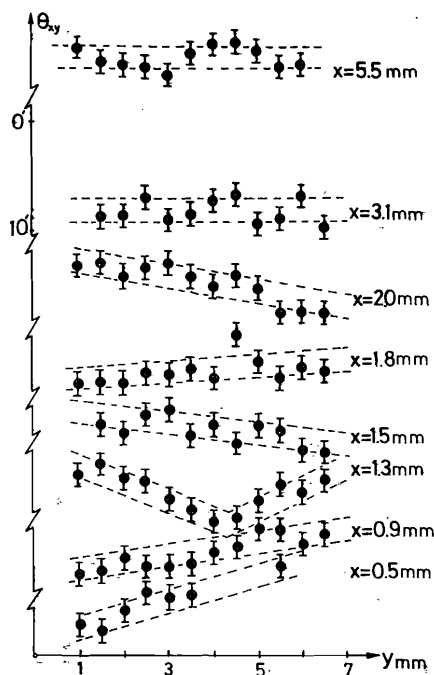
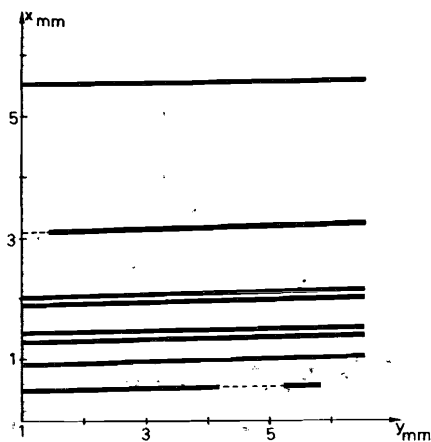
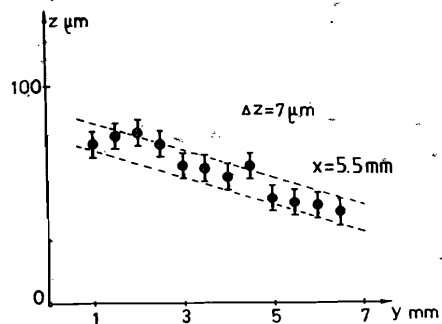


Fig.21. The results of the measurements of orientation angle θ_{xy} for these 8 particle tracks.

Fig.22. The results of the measurements of the z-coordinate for a particle track with $X = 1.8$ mm.



along the scanning lines was 0.02 mm. The time of scanning of the whole area was about 40 minutes and 207 pictures were collected.

After the first evaluation 45 pictures turned out to be "wrong". In most cases they were pictures of real tracks going at such angles θ_{xy} , θ_z that one of two meso-optical images already is out of the frame of the CCD matrix. Thus we had 162 pictures said to be signals of real tracks. According to the results of the second evaluation step, these pictures correspond to 8 real tracks. All the tracks found by the computer controlled MFTM were really observed in this area by a traditional optical microscope. The positions of these 8 real tracks are shown in fig.20.

The results of the measurements of the orientation angle θ_{xy} for 8 real tracks are given in fig.21. The variations of θ_{xy} along Y-axis are induced by the microscopic distortions of the nuclear emulsion volume as a result of the photochemical treatment of the nuclear emulsion layer 0.6 mm deep. The detectable curvature radius of the macroscopic distortions is of the order of 10 m or less. It must be noticed that in the case when the particle track undergoes the scattering in some point as the result of the nuclear interaction the function $\theta_{xy}(Y)$ will show a jump. Therefore the smooth variations of this function can be interpreted as variations of the macroscopic distortions. The particle track with $X = 1.3$ mm shows a strong variation of curvature radius with sign reverse. From fig.21 we see that the variance of the θ_{xy} measurements is equal to $\Delta\theta_{xy} = \pm 1'$.

The dependence $z(Y)$ for the particle track with $X = 1.8$ mm is given in fig.22. The variance of the z coordinate measurements is equal to $\Delta z = \pm 7 \mu\text{m}$. The measurement error for θ_z , estimated in the same way is $\Delta\theta_z = \pm 10'$.

PERFORMANCES OF THE COMPUTER CONTROLLED MFTM

The experimental tests described in this paper and the results obtained in the previous works, ref. /13,18,19/, can be summed up if we give the performance of the computer controlled MFTM.

Spatial resolution. The spatial resolution along the radial coordinate across the particle track is equal to $\Delta\rho = \pm 1 \mu\text{m}$. The sagittal spatial resolution that is the measurement error of the coordinate of the point where the particle track is ended in the fields of view of the MFTM is equal

to $\Delta l = \pm 30 \mu\text{m}^{/13/}$. The spatial resolution along the z -coordinate is equal to $\Delta z = \pm 10 \mu\text{m}$.

Angular resolution. The error with which angle θ_{xy} can be estimated by the MFTM is equal to $\Delta\theta_{xy} = \pm 1'$, and $\Delta\theta_z = \pm 10'$ for angle θ_z .

Selectivity. The accepted angular interval $\delta\theta_{xy} = \pm 1^\circ$. The MFTM does not "see" the particle tracks with orientations out of this chosen angular interval. The intensity of the X-ray marked grid of the width $\approx 10 \mu\text{m}$ is suppressed by the MFTM in the ratio 1:360^{/18/}.

Aberrations. The coma aberrations in the MFTM is no more than $\pm 1 \mu\text{m}$ over the field of view $0.4 \times 0.4 \text{ mm}^{/13/}$.

Macroscopic distortions. The curvature of the particle tracks induced by the macroscopic distortions of the nuclear emulsion medium which can be detected by the MFTM is of the order of 20 m over the length 6 mm or 10" (angular seconds) over the field of view (0.7 mm).

Rapidity. The time of the measurement is 30 ms. The time of search of the area $6 \times 6 \text{ mm}^2$ is 40 minute. As the number of the particle tracks found is 8, the rapidity of search is of the order of 4.3 cm^2 per hour or 100:1 faster than for manual search, 1 cm^2 per day with probability of success 0.3.

The time resolution of the electronics allows an increase in the velocity of X-Y stage in the ratio 3:1.

CONCLUSIONS

The Mesooptical Fourier Transform Microscope (MFTM) controlled by the computer was built in JINR (Dubna). This new experimental device can be used in high energy physics for automatic search of particle tracks with predetermined parameters in nuclear emulsion layers. The device was tested on particle tracks of the high ionization level. The automatic evaluation of nuclear emulsion was performed for the first time without any mechanical or electronical depth scanning. Owing to this improvement and to the instant angular selectivity the speed of search which can be attained with the MFTM is at least two orders of magnitude higher than for systems with a traditional optical microscope.

ACKNOWLEDGEMENTS

The authors express many thanks to the corresponding member of the Academy of Sciences of the USSR V.P.Dzheleпов,

Director of the Laboratory of Nuclear Problems, Joint Institute for Nuclear Research (Dubna), for supporting the investigations in mesooptic for many years and to Prof. S.A.Bunyatov, Chief of the project Neutrino Detector, for leadership in the work on the MFTM. The development of the MFTM is accomplished as part of the USSR - Hungary scientific collaboration, with the support of Prof. D.Kiss (KFKI, Budapest) to whom the authors express their cardinal gratitude.

REFERENCES

1. Sacton J. - Proceedings of the conference on "Search for Charm, Beauty and Truth at High Energies", Erice, Italy, N.Y., Plenum Press, 1984, p.169.
2. Arthur A.A. et al. - LBL Communications, No.16870; IEEE Trans.Nucl.Sci., 1983, vol.30, No.5, p.3779.
3. Niu K. - "XX International Conference on High Energy Physics", Madison, Wisconsin, 1980, Proc., Part 1, p.352, American Institute of Physics; N.Y., 1981.
4. Dameri M. et al. - Proceedings of the Istituto Nazionale di Fisica Nucleare, INFN/TC-84/28, Genova, 1984. CERN Courier, June 1983, p.184.
5. Soroko L.M. USSR patent No.743424 12.12.1978, Published 1981, Bull. No.21, p.262.
6. Astakhov A.Ya., Soroko L.M. - JINR Communication, P13-83-119, Dubna, 1983.
7. Astakhov A.Ya., Soroko L.M. - JINR Communication, P13-83-120, Dubna, 1983.
8. Astakhov A.Ya. et al. - JINR Communication, P13-84-277, Dubna, 1984.
9. Bencze Gy.L., Soroko L.M. - JINR Preprint, E13-84-310, Dubna, 1984, submitted to ICO-Congress, Sapporo, Japan, 1984.
10. Astakhov A.Ya. et al. - JINR Communication, P13-85-378, Dubna, 1985.
11. Bencze Gy.L. et al. - JINR Communication, P13-86-630, Dubna, 1986.
12. Astakhov A.Ya. et al. - JINR Communication, P10-87-275, Dubna, 1987.
13. Bencze Gy.L., Soroko L.M. - JINR Communication, P13-86-659, Dubna, 1986.

14. Soroko L.M. - JINR Preprint, E13-87-292, Dubna, 1987.
15. Bencze Gy.L., Soroko L.M. - JINR Communication, E13-87-387, Dubna, 1987.
16. Bencze Gy.L., Soroko L.M. - JINR Communication, E13-87-388, Dubna, 1987.
17. Bencze Gy.L., Soroko L.M. - JINR Communication, E13-87-389, Dubna, 1987.
18. Bencze Gy.L., Soroko L.M. - JINR Communication, P13-87-594, Dubna, 1987.
19. Soroko L.M. - JINR Communication, P13-87-527, Dubna, 1987.
20. Soroko L.M. - JINR Communication, D1-82-642, Dubna, 1982.
21. Soroko L.M. - JINR Communication, P13-87-468, Dubna, 1987.
22. Soroko L.M. - JINR Communication, P13-87-576, Dubna, 1987.
23. Nussenzveig H.M. - Causality and Dispersion Relations, Academic Press, New York, 1972.
24. Bencze Gy.L., Soroko L.M. - JINR Communication, P13-86-240, Dubna, 1986.
25. Bencze Gy.L. et al. USSR Patent No.1.402.981. Published 1988, Bull. No.22, p.159.
26. Soroko L.M. - JINR Communication, P13-87-170, Dubna, 1987.
27. Soroko L.M. - JINR Communication, P13-87-169, Dubna, 1987.
28. Bencze Gy.L., Soroko L.M. - JINR Communication, P13-85-502, Dubna, 1985.
29. Soroko L.M. - JINR Communication, P13-87-358, Dubna, 1987.
30. Batusov Yu.A., Bencze Gy.L., Soroko L.M. - JINR Preprint, E13-88-729, Dubna, 1988.

Received by Publishing Department
on December 23, 1988.

Астахов А.Л. и др. E13-88-892
Мезооптический фурье-микроскоп - новое устройство
для физики высоких энергий

Описан мезооптический фурье-микроскоп /МФМ/ - новое устройство для физики частиц высоких энергий. МФМ предназначен для наблюдения прямых следов частиц в ядерной фотоэмульсии. МФМ работает без какого-либо сканирования по глубине, механического или электронного, и может рассматриваться как селективно видящий "глаз". Приведена система, которая содержит МФМ в качестве основного узла и которая управляется от компьютера. Указанная система может быть использована для быстрого поиска следов частиц и событий, образованных нейтрино высоких энергий от ускорителя. Приведены результаты первого экспериментального испытания МФМ, управляемого от компьютера. Описаны и обсуждены технические характеристики этой системы. Показано, что угловое разрешение МФМ равно одной угловой минуте, а время измерения равно 30 мс. Так как все операции в МФМ происходят без какого-либо сканирования по глубине, то эта новая система просмотра работает по крайней мере в 100 раз быстрее, чем любая из известных систем с использованием традиционного оптического микроскопа.

Работа выполнена в Лаборатории ядерных проблем ОИЯИ.

Препринт Объединенного института ядерных исследований. Дубна 1988

Astakhov A.Ya. et al. E13-88-892
Mesooptical Fourier Transform Microscope - a New Device
for High Energy Physics

A new device for high energy physics, Mesooptical Fourier Transform Microscope /MFTM/, designed for observation of straight line particle tracks in nuclear research emulsion is described. The MFTM works without any mechanical or electrical depth scanning and can be considered as a selectively viewing "eye". The computer controlled system containing MFTM as the main unit is given. This system can be used for fast search for particle tracks and events produced by high energy neutrinos from particle accelerators. The results of the first experimental test of the computer controlled MFTM are presented. The performances of this system are described and discussed. It is shown that the angular resolution of the MFTM is 1 angular minute and the measurement time is equal to 30 ms. As all operations in the MFTM go without any depth scanning this new evaluation system works at least two orders of magnitude faster than any known system with a traditional optical microscope.

The investigation has been performed at the Laboratory of Nuclear Problems, JINR.

Preprint of the Joint Institute for Nuclear Research. Dubna 1988